FULL-LENGTH ARTICLE

The First Ground-Based Measurement of Atmospheric Carbonyl Sulphide over Addis Ababa (Ethiopia)

Milkessa G. Homa[1*], Gizaw M. Tsidu[2], Tamirat A. Desta[1]

[1]Jimma University, College of Natural Sciences, Physics Department
[2] Botswana International University of Technology and Science (BIUTS), College of Science, Department of Earth and Environmental Sciences, Palapye, Botswana.

***Corresponding Author**: mikemen.homa@gmail.com

ABSTRACT

Measurement of Carbonyl sulphide is very crucial to estimate the sulfur budget and is used as a tracer for the carbon cycle. Its simultaneous consumption with CO_2 during photosynthesis by plant uptake makes it an ideal candidate for the partitioning of photosynthesis from respiration. This research provides the first ground-based abundance of OCS from a high-resolution Fourier Transform Infrared spectrometer over Addis Ababa (9^{o}1$^{'}$N, 38^{o}76$^{'}$E, an altitude of 2443 m.a.s.l.). We used PROFFIT95 to retrieve the vertical profile, average tropospheric and stratospheric mixing ratios, and column amount from the solar absorption spectra of OCS. Analysis of random and systematic error to retrieval shows that the total error contribution due to atmospheric and auxiliary parameters is less than 10%. The tropospheric and stratospheric average VMR in our site is 0.488 ppbv and 0.230 ppbv, respectively, with deviation from the global mean by 2.4% for tropospheric mixing ratio. The hourly variation of OCS particularly on 14, March 2010 shows slight accession from mid-morning to noon and reduction in the afternoon with a change in VMR of 0.019 ppbv. The tropospheric volume mixing ratio (in the unit of parts per billion by volume) and total column amount time series result from May 2009 to April 2010 show seasonal variation with maximum (0.60) in May and June, and minimum (0.37) in December and January. The total column amount reaches up to $8.5X10^{19}$ molecules/m^2. The correlation between stratospheric tropopause level and the accession of stratospheric OCS level during hot season worth detail investigation to understand the variation of OCS besides taking long term measurement for trend analysis.

Keywords: ILS; Partial Column; Time Series; Total Column; Vertical profile

INTRODUCTION

Carbonyl sulphide (OCS) is a major sulphur reservoir in the troposphere, on a global scale (Barkley et al., 2008). Its main sources are biomass burning, soil, wetlands, oxidation of carbon disulphide (CS_2) and dimethyl sulfide (CH_3SCH_3 or DMS), volcanic eruptions, industrial uses, automobiles, oceans, etc. (Schneider, 2002; Seinfeld and Pandis, 2006). Atmospheric oxidation of reduced sulphur gases, in particular DMS and CS_2, also produces OCS. There are also anthropogenic sources of direct and indirect (oxidation of CS_2 released by industry and natural gases) contribution to atmospheric OCS significantly (Chin and Davis, 1993; Watts, 2000) and from biomass burning (Crutzen et al., 1979; Brühl et al., 2012). The direct contribution by biomass burning accounts for 10 - 20 % of the overall sources (Notholt et al., 2003); also soil and wetlands contribute to the OCS budget (Kettle et al., 2002). Anthropogenic emissions almost entirely consisting of SO_2, come from coal-burning and sulphide ore smelting. They are responsible for the emission of 80 Tg S per year according to Butcher et al. (1992). Vegetation, soil uptake, and hydroxyl radical reaction are the main sinks of OCS in the lower troposphere (Kettle et al., 2002). A plant can take up OCS through the stomata and assimilate it even more efficiently than CO_2 (Sandoval-Soto et al., 2005). The biological processes involved are dependent on temperature and humidity, which gives rise to strong diurnal and seasonal cycles of OCS, especially in middle and high latitudes (Kettle et al., 2002). Especially during the night, when the plant stomata are closed, oxic soils can be an important sink for atmospheric OCS (Kuhn et al., 2000; Steinbacher et al., 2004). Photodissociation breakdown through the absorption of ultraviolet sunlight in stratosphere can be a sink mechanism for this gas (Crutzen, 1976; Turco et al., 1980).

Carbonyl sulphide is considered as a component of the atmosphere at a tropospheric concentration of approximately 500 parts per trillion (ppt) or 0.5 parts per billion (ppb) by volume, corresponding to a global burden of 2.4 million tons; but enhanced OCS mixing ratios of up to 0.6 ppbv from biomass burning emissions have been found below the tropical tropopause at altitudes between 10 and 18 km (Seinfeld and Pandis, 2006). The average total worldwide release of OCS to the atmosphere has been estimated at 3 million tons per year (Main and Davis, 1995). It is the only sulphur compound that survives to enter the stratosphere (through tropical tropopause) except SO_2 which is directly injected into the stratosphere during volcanic eruptions. Owing to its long lifetime of about (2-6 years) OCS is transported to the stratosphere where it is either photo dissociated by UV radiation or reacts with atomic oxygen or OH radical, to ultimately form sulphate aerosol particles (Jung layer) that influence the Earth’s radiation budget and stratospheric ozone chemistry (reduction in stratospheric ozone concentration) (Barkley et al., 2008). The stratospheric sulphate aerosol, in turn, reflects incoming shortwave solar radiation (affecting Earth’s radiation budget), as a result of cooling the climate system (Brühl et al., 2012; Kremser et al., 2015) during volcanically quiescent periods. Out of the total estimated OCS quantity (5.2 Tg) in the atmosphere, 4.63 Tg is in the troposphere and 0.57 Tg in the stratosphere (Main and Davis, 1995; Seinfeld and Pandis, 2006). In the atmosphere, the hydroxyl radical HO* initiates the oxidation of OCS and carbon disulphide (CS_2) and result in a yield of 8 - 12 million tons as sulphur (S) in atmospheric sulphur dioxide per year. Its photo-oxidation produces sulphur dioxide which later converts to the background aerosol of hydrated sulphuric acid. This is the cause of acid rain which results in deforestation and ultimately climate change (Homa et al., 2017). The photo-oxidation of OCS has a contribution in reducing the number of ozone concentrations in the stratosphere.

OCS has attracted attention for its contribution to the non-volcanic background stratospheric sulphate aerosol (SSA) layer and more recently for its potential to become a photosynthesis tracer. Unlike CO_2, which involves in both photosynthesis and respiration, OCS is involved only in photosynthesis by plant uptake, making OCS an ideal candidate for partitioning the photosynthetic uptake from respiration and thus helping constrain gross primary production (GPP) (Montzka et al., 2007; Campbell et al., 2008; Asaf et al., 2013; Berry et al., 2013). Accurate knowledge of the global OCS budget will thus help better understand the global sulfur and carbon cycles. However, large uncertainties remain in the field of OCS research, e.g., its global mass budget, its relative contribution to SSA, or the impact of anthropogenic emissions on its long-term trend (Lejeune, 2016). To minimize the uncertainties, more continuous measurement of OCS either from space like the TES board on Aura (Kuai et al., 2015) or ground-based networks like NDACC (network for detection of atmospheric composition change) is highly important especially in lower latitude area where there is a scarcity of measuring facilities.

High-resolution Fourier Transform Infrared (FTIR) spectrometer installed at Addis Ababa through a collaboration of the Institute for meteorology and climate research (IMK) and the Department of physics of Addis Ababa University is the first of its kind to measure continuously in Africa and widely used to measure spectra of trace atmospheric gases in the region. Hence, it is expected to provide unique information about equatorial African atmospheric trace gases profile, column amounts, and time series of nearly a year from May 2009 to April 2010. The main goal of this work is to assess the vertical profile, partial/total column amount, particle column concentration, mean tropospheric and stratospheric VMR, and time series of atmospheric OCS in the region using ground-based high-resolution FTIR spectrometer for a duration of nearly a year (May 2009 - April 2010) for the first time.

MATERIALS AND METHODS

The Bruker IFS 120M instrument FTIR spectrometer was installed at a tropical site located in Addis Ababa, Capital of Ethiopia ($9^{o}1^{'}$N, $38^{o}76^{'}$E, an altitude of 2443 m.a.s.l.) which has been continuously measuring several atmospheric trace gases since May 2009. The measured spectra from May 2009 to

April 2010 were analysed to retrieve vertical profiles and total column amount of OCS in the region. The retrieval code used in this study is PROFFIT (stands for PROFileFIT) developed by Haze (2000). The main steps in the retrieval can be divided into two parts generally: first, the forward calculation (PROFFWD) which provides synthetic and measured spectrum and derivatives for error estimation. In this part, the software performs a radiative transfer calculation for a given set of relevant atmospheric parameters (temperature-T, pressure-p, volume mixing ratio-VMR) and auxiliary parameters (SZA, ILS) input quantities for the spectral microwindows selected for analysis. The apriori data is from WCCAM and the T, p data is from Goddard. The derivative of the spectrum with respect to the target and auxiliary quantities are allowed to vary in the process of searching for the best estimate of the atmospheric state; second, the inversion model (PROFFIT), which processes the PROFFWD model output and suggests an improved solution, restarts forward model with updated variables, cycles until convergence is reached. In short, PROFFIT determines the best estimate of the observed atmospheric state by improving fit quality to the recorded spectrum iteratively. PROFFIT allows us to choose between two regularization methods: the Optimal Estimation (OE) and the Tikhonov-Phillips (TP) Methods (Twomy, 1977; Rodgers, 2004). We have used the TP method, which additionally enables us to impose two kinds of constraints-absolute regularization or slope regularization of a start profile and the retrieved profile. Fig. 1 shows the HBr spectral fit for the indicated wavenumber region of the measurement on 1st June 2009. The upper panel is a plot of the measured and calculated transmission spectra and the lower panel is the residual between the two spectra with a resolution of 0.008cm^{-1}. The root-mean-squared (RMS) value of the noise is below 1% and it is comparable to the result reported by Haze et al. (1999). We can infer from the figure that the residual is random noise.

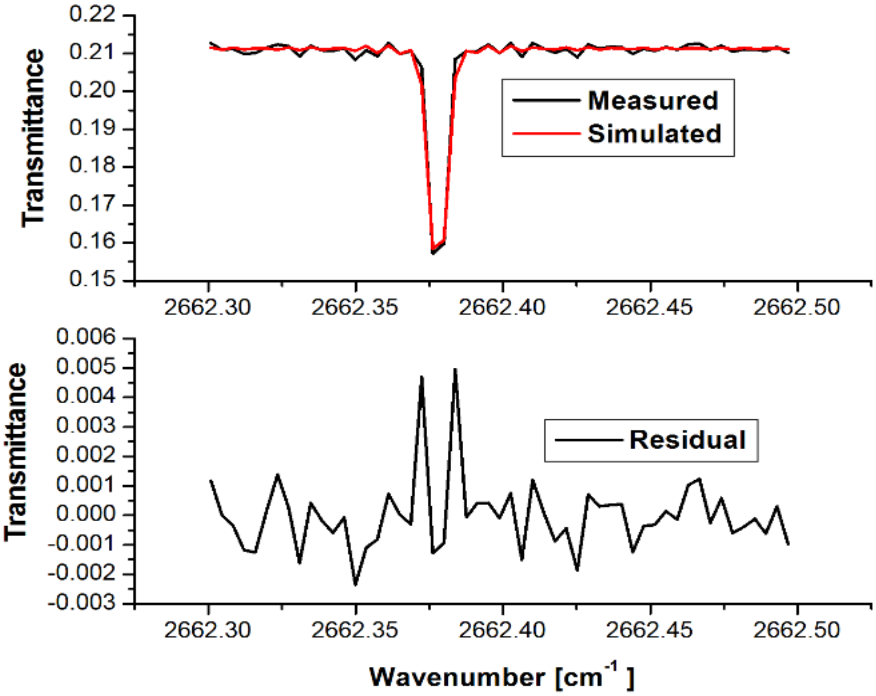

Fig. 1. The measured and simulated spectral fit with the corresponding residual spectra for the date of 01 June 2009.

The retrieved ILS of our IFS120M for the HBr cell measurement taken on 01, June 2009, whose spectral fit is shown in Fig.1, is kept to retrieve the required atmospheric trace gases. The tropospheric trace gas total column retrieval is relatively insensitive (< 1%) to realistic distortions of the ILS from ideal. But for stratospheric gases, realistic distortion of the ILS may modify retrieved total columns by amounts of up to 3% (Griffith et al., 2003). The modulation efficiency loss and phase error are calculated using LINEFIT12 software developed by Haze (1999). Fig. 2 shows the variation of modulation efficiency (ME) loss of our IFS120M instrument since the beginning of measurement days. The ME loss and phase error as a function of optical path difference (OPD) are then calculated using the software such that the residual between the retrieved and the measured spectra is minimized. The declination of modulation efficiency at maximum OPD on May 8 2009, is less than 6% and on Jan. 14, 2010 the declination in modulation efficiency at maximum OPD is less than 2%. This shows that the instrument's alignment has improved since the beginning of the measurement days.

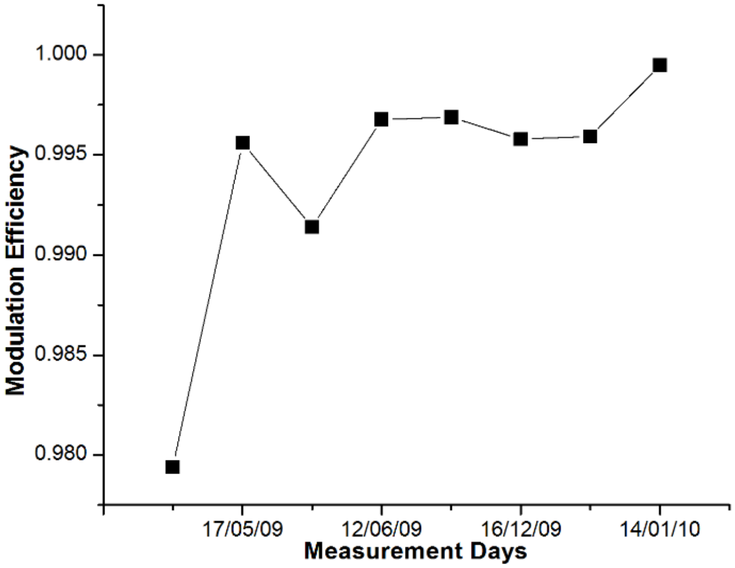

Fig. 2. Evolution of modulation efficiency loss

The other parameter which characterizes the instrumental line shape is the phase error. Fig.3 shows the variation of phase error with time. Taking the phase error into account in the calculated spectra to fit the measured spectra helps to correct the effect of the zero-offset.

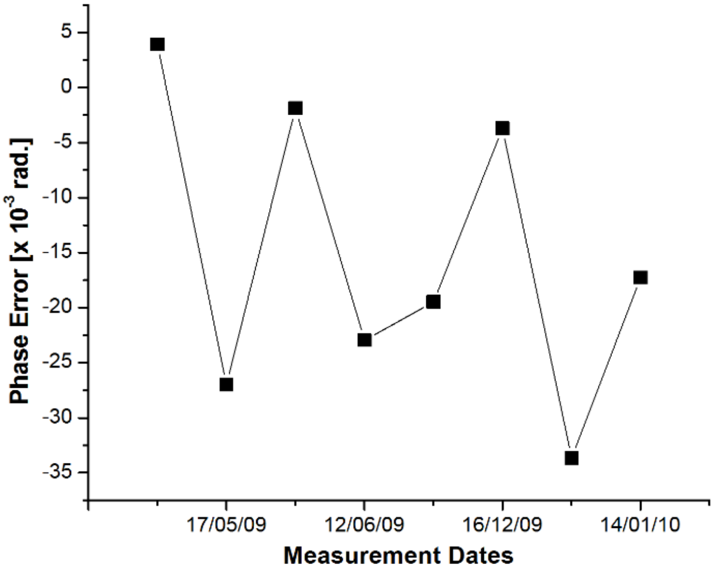

Fig. 3. Evolution of phase error

Hence, phase error affects the retrieved total columns in two separate ways; first, through the change in line shape of the actual absorption line and second, through a change in the effective continuum level at the centre of the absorption line nearby, whose wings overlap the narrow line of interest. In the latter case, the phase error distorts the strong band and affects the local zero and continuum levels in the observed spectrum.

SENSITIVITY ANALYSIS

The other parameter worth discussing is the averaging kernel matrix which is the measure of the sensitivity of the retrieved state to the true state at different heights. The kernel also helps to determine the independent layers of the stratified atmosphere. The plot of the rows of the averaging kernel matrix for some selected heights is shown in Fig. 4 for a profile retrieval of OCS consisting of 41 levels (height grids) assumed by the code. The graph also shows the different sensitivity of the retrieval in tropospheric and stratospheric regions. According to Wiacek et al. (2007), the integrated area under each averaging kernel is a simple measure of the amount of non-apriori information that appears in the retrieval at the corresponding height.

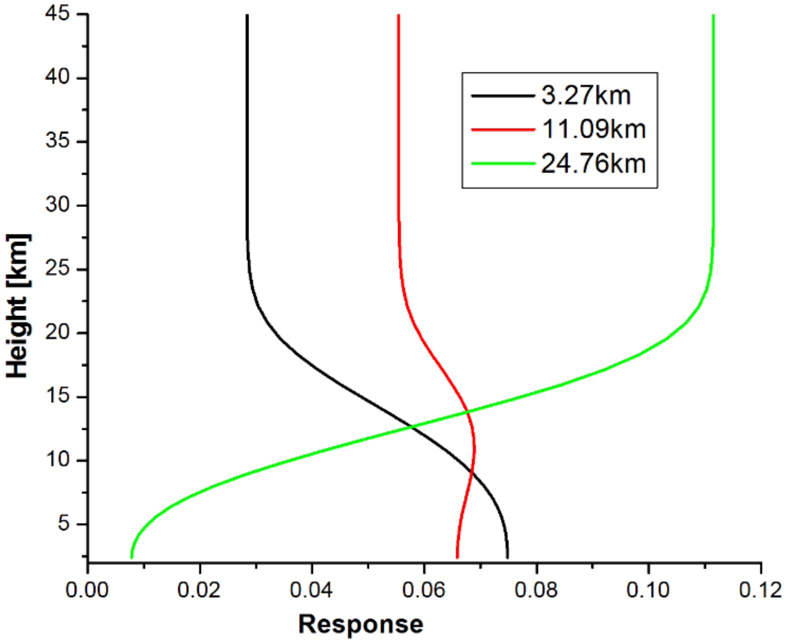

Fig. 4. Averaging Kernel for selected heights

Since the mean tropopause height over Ethiopia is above 17 km (the daily NASA/Goddard meteorological data) the averaging kernel tells us that the gaseous OCS is dominantly a tropospheric gas.

OCS SPECTRAL SIGNATURE (MICRO-WINDOW SELECTION) IN MID INFRARED

For the retrieval of OCS, we used different microwindows in the spectral range of 2038.8 to 2051.5 cm^{-1} (Table 1). The optimum microwindows are used by different authors (Notholt, et al., 2006, Schneider, 2002). Spectral parameters of OCS and interfering species are from HITRAN 08 and HITRAN 04.

Table 1. Microwindows of OCS and interfering species

Microwindow (cm^{-1})	Main interfering species
2038.90000-2039.08056	H_2O, CO_2, O_3, CO
2045.48000-2045.66000	H_2O, CO_2, O_3, CO
2047.80000-2048.70000	H_2O, CO_2, O_3, CO
2049.30305-2050.11500	H_2O, CO_2, O_3, CO
2051.20000-2051.50000	H_2O, CO_2, O_3, CO

The microwindows used in this research contain an optimized spectral band of the target and the interfering species. These microwindows are the regions where the effect of interfering species is reduced and the PROFFIT software retrieves OCS from the average contribution of these spectra.

Fig.5 shows the spectral fit between the measured and calculated spectra for one of the microwindows in Table 1. The target (OCS) and the interfering species (ozone, carbon dioxide, and carbon monoxide) in this band are identified. The lower panel of the figure shows the residual (the difference between the measured and calculated) spectra. The maximum percentage error for the spectral fit shown in Fig.5 is less than 1%.

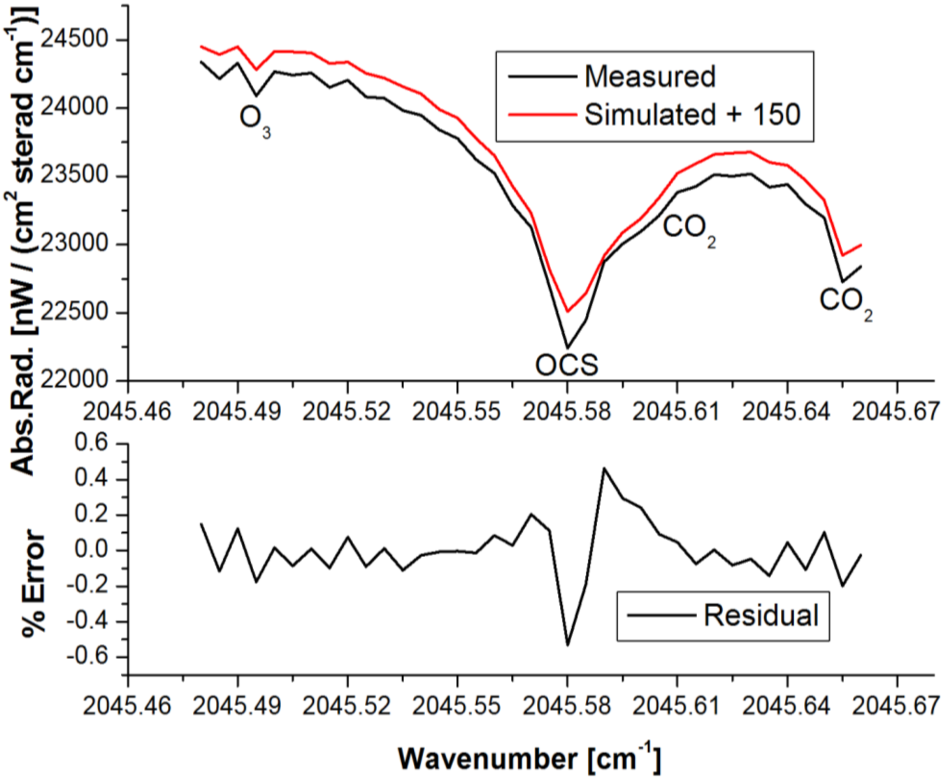

Fig. 5. Measured and calculated spectra

In all microwindows used for the retrieval of OCS, the maximum percentage error is less than 2%, which is less than the 4% error reported by Sung et al. (2007), and it assures good retrieval results in this work. The noise in Fig. 5 is dominantly random except for some systematic features near the peak positions of the target and interfering species.

ERROR ANALYSIS

PROFFIT allows error estimation. The percentage of both random and systematic errors for selected heights is shown in Table 2 and Table 3 respectively. The ILS (ME loss), line of sight (LOS), and solar line errors are very small as compared to the rest. The spectral noise is due to the uncertainty of the depth of the absorption line with respect to its surrounding continuum, which is proportional to the uncertainty of the line strength.

Table 2. Percentage random (statistical) error of OCS

Height (km)	Baseline	ILS	LOS	Solar	Noise	Total Stat.
2.43	1.983	0.0589655	0.051471	0.0737471	1.601	2.611
6.38	1.883	0.0551396	0.051462	0.0972308	1.367	2.377
12.71	1.770	0.0236456	0.051495	0.1290000	0.747	1.939
18.31	1.982	0.0950629	0.051507	0.0793022	1.846	2.775
36.34	2.086	0.1320000	0.051519	0.0454829	2.464	3.319

Where: Baseline, refers to spectral baseline error; ILS, instrumental line shape error; LOS, line of sight error; Solar, refers to solar line error; Noise, is instrumental noise.

An offset signal in the spectrum may be mainly due to the nonlinearity of the detector. The offset typical value of InSb (Indium Antimonide) detector is 1% of the continuum signal. The spectroscopic data error is due to spectroscopic parameters such as line intensity and gamma values. Spectroscopic errors lead to systematic deviations from a real profile and column amounts.

Table 3. Percentage systematic error of OCS; Where: Temp, is temperature error; Spec, refers to spectroscopic error from HITRAN data.

Height (km)	Baseline	ILS	LOS	Solar	Temp	Spec.	Total Syst.
2.43	1.983	0.058966	0.0057195	0.018437	0.240	2.071	2.878
6.38	1.883	0.055140	0.0057100	0.024302	0.202	2.085	2.818
12.71	1.770	0.023646	0.0057202	0.032140	0.095	4.954	5.262
18.31	1.982	0.095063	0.0057228	0.019828	0.251	8.452	8.687
36.34	2.086	0.132000	0.0057243	0.011371	0.324	0.324	9.930

The ILS influences the result by modifying the shape of the VMR profile, especially at altitudes where the Doppler broadening is significant (above 20 km) (Schneider, 2002). The temperature uncertainty also influences both the column amount and shape of the profile. Another parameter that influences the simulated spectrum by the radiative transfer code is the solar zenith angle (SZA) or line of sight (LOS). We use the SZA corresponding to the meantime of measurement ($\frac{t_{start}+t_{end}}{2}$) in the radiative transfer code, where t is scanning time. The detail of error estimation is found in Haze (2000) and Schneider (2002). The LOS, which significantly affects the retrieval in low latitude areas is less than 0.1%. In general, the random and statistical error contributions of both atmospheric and auxiliary parameters are less than 10% of which 9.7 % is the spectroscopic error from systematic contribution while the total random error (without temperature error) is less than 4% at the 36.34 km. The percentage errors for both random and systematic contributions are less than the results reported in various literature (Rhineland et al., 1992; Lejeune et al., 2016).

RESULTS

The vertical profile of OCS for solar attenuated spectra measured by the FTIR spectrometer is retrieved in the 5th NDACC filter band, in the microwindows region given in Table 1. In these microwindows regions, there are additional H_2O, CO_2, O_3, and CO features that interfere with the target species. All spectroscopic parameters for retrieval of OCS and H_2O are taken from HITRAN08 while for the rest HITAN04 (Rothman et al., 2009; 2005) were utilized. We used the slope regularization method for the retrieval of the OCS profile, while the signature of other species is calculated by a simple scaling of the start profile. The tropospheric VMR is nearly constant while the stratospheric one shows steadily decreasing (Fig. 6).

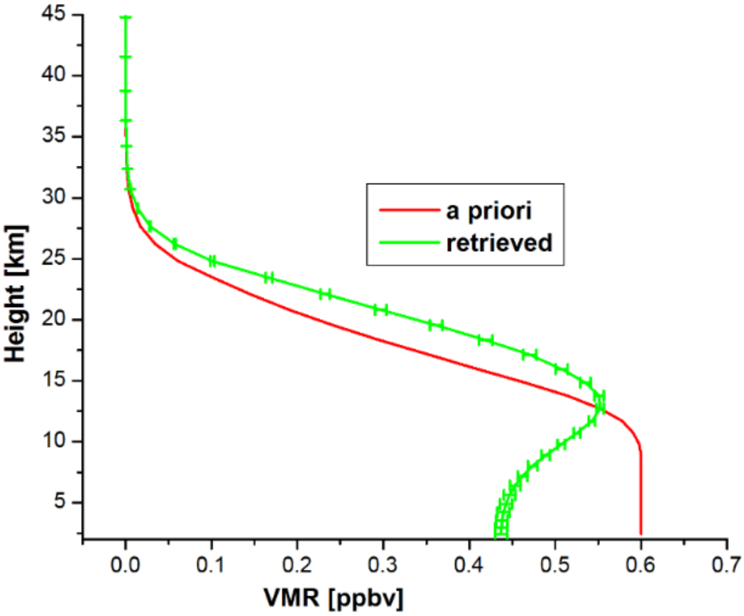

Fig. 6. Mean retrieved profile of OCS

The time variation of OCS VMR for a particular day is shown in Fig. 7. The measurement was taken on 14 March 2010 starting from 9:03 a.m. to 1:35 p.m. local time. The time axis on this plot is in universal time (UT) where Addis Ababa is 3 hrs. ahead.

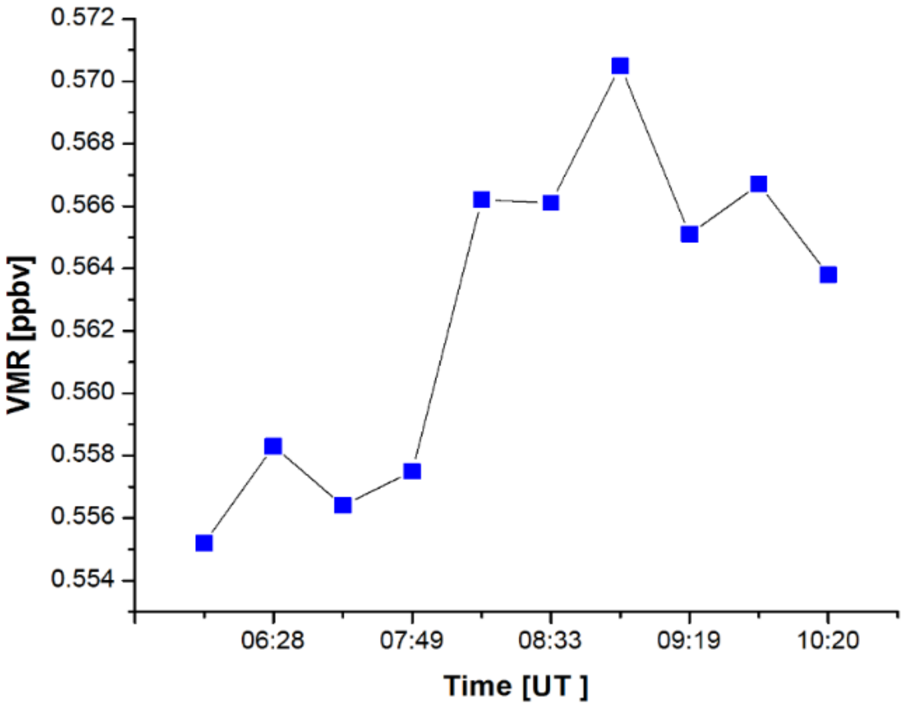

Figure 7. Variation of OCS VMR with time

The maximum VMR is observed during noon and minimum before and after noon time and this result helps to see the hourly variation of OCS from morning to afternoon during which different biospheric activities take place but the difference between peak and trough is not high in this case.

The partial column and the integrated (total) columns of OCS are important to estimate the mixing ratio of trace gases in different atmospheric regions. The partial and total columns of OCS for a particular date is shown in Fig.8.

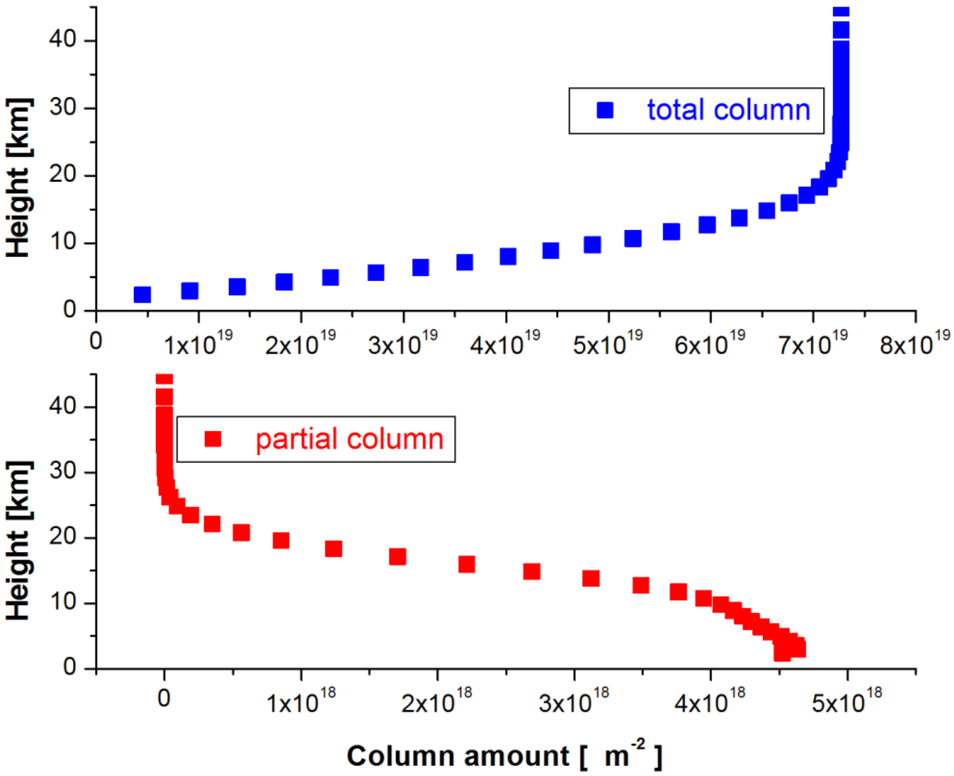

Fig. 8. Partial and integrated columns of OCS on the 27 January 2010.

The upper and lower panels of Fig. 8 show the vertical distribution of the gas as well as the level at which the high and low concentrations are found for the date mentioned. The total column is the integration of the partial column amount of each of the 41 levels assumed by the forward model (PROFFWD). The result shows a negligible contribution to the partial column after 30 km.

The data at hand considered for this study is limited to a few measurement days compared to nearly a year's time period. However, we tried to see the time series of total column OCS for 49 measurement days since the first date of continuous operation of the FTIR spectrometer at Addis Ababa rejecting bad measurements (due to shades and cloud cover mostly) from May 2009 to April 2010 (Fig. 9).

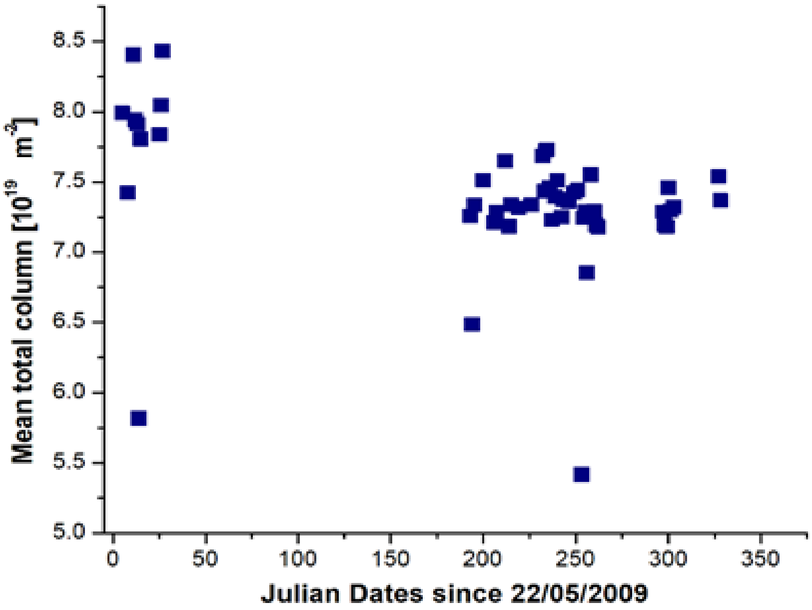

Fig. 9. Time series of total column OCS.

The limited number of measurements within this period is due to unaffordable natural phenomena of the rainy season (from the middle of June to late September) and unexpected cloud cover over Addis Ababa which severely limited the observing capability of the instrument during this period. The InSb detector failure was also a reason for not taking continuous measurements.

The partial and column amount of OCS also show variation with season though we don't have sufficient data to see a long period fluctuation and trend in our region. The total column amount tends to decrease from May to April in the troposphere while it tends to increase in the stratosphere as shown in Fig. 10 for the measurement period.

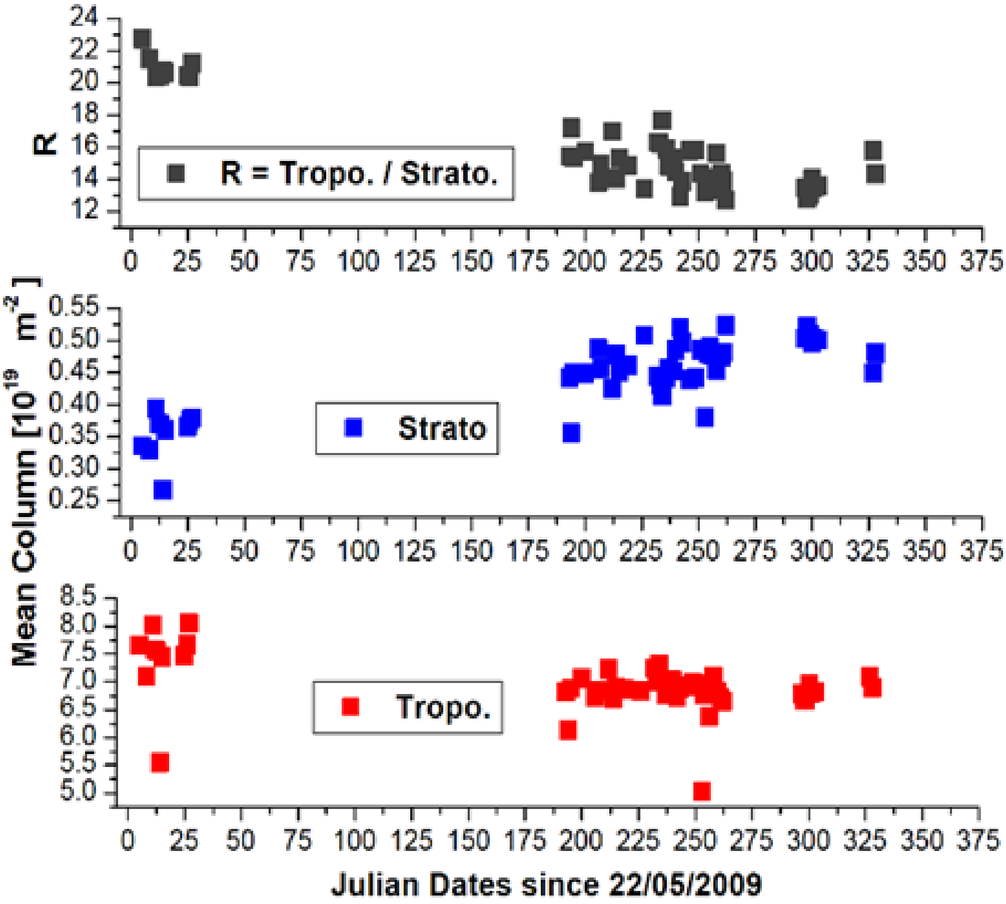

Fig. 10. Time series of tropospheric and stratospheric total column OCS.

The upper panel is the ratio between tropospheric and stratospheric total column amount and tends to decrease.

In addition to the time series of column amount, the vertical profile time series of OCS VMR from May 2009 to April 2010 of OCS measurement is shown in Fig.11. The mixing ratio of OCS also shows a slight enhancement up to 0.6 ppbv (from late May to the middle of June 2009) which is higher than the mean 0.45 ppbv - 0.5 ppbv in the troposphere.

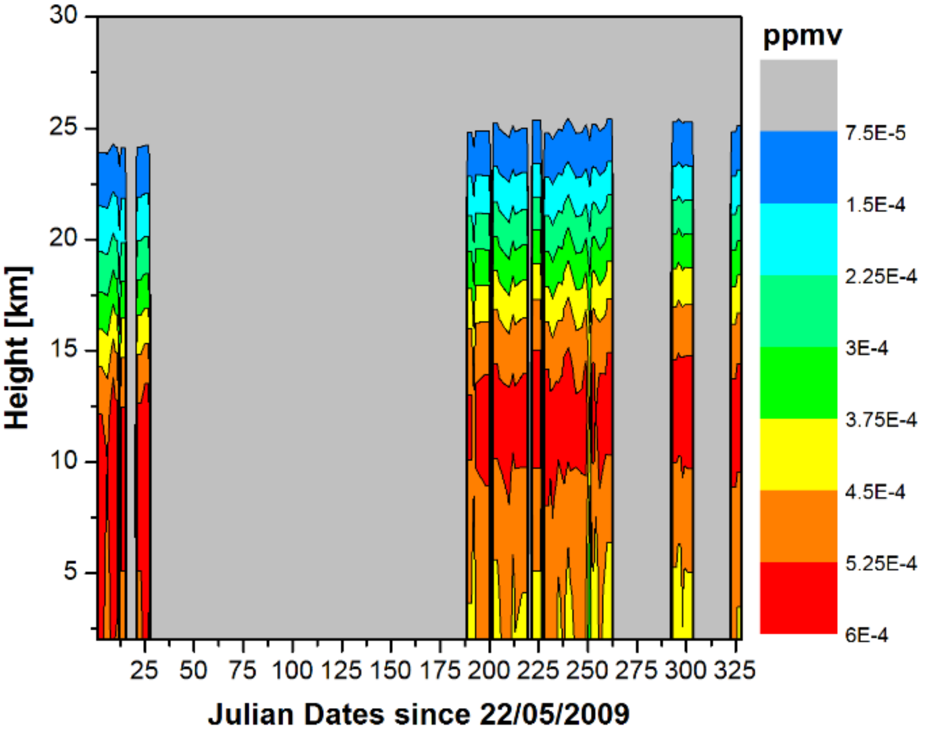

Fig. 11. Time series of the vertical profile of OCS.

As indicated in this figure the mixing ratio reaches up to 0.6 ppbv and steadily decreases in the stratosphere. The grey background in Fig. 11 indicates the non-measurement days hence zero VMR values of OCS. The daily variation of OCS can also be seen from the same plot. The reduced VMR value closer to the surface (yellow colour) is due to interfering species and supported by Rhineland et al. (2008).

DISCUSSION

The OCS vertical profile (Fig. 6) shows a minor slope from 0.55 ppbv about nearly 13 km to 0.45 ppbv at the observation site, 2.443 km. This slope from nearly 13 km to 2.443 km could be due to interferences with the CO_2 line about wavenumber 2045.60 cm^{-1} and unknown interfering line. A similar gradient in tropospheric OCS amount is reported by Johnson et al. (1993) and Schneider, (2002). The profile of OCS shows that the VMR of OCS is rapidly decreasing with altitude above 15 km. It declines from 0.55 ppbv in the troposphere to less than 0.25 ppbv at 20 km. The standard deviation of the retrieved profile is shown in the same figure as the error bar having a magnitude between 6.964×10^{-10} at the observation site to 4.536×10^{-10} at 85 km. The OCS profile at the tropical tropopause can reach levels comparable to the lower tropospheric mixing ratios most likely as a result of convective uplift of biomass burning plumes and tropopause height. This is supported by other researchers (Engel and Schmidt, 1994; Chin and Davis, 1995).

Fig. 7 shows the hourly variation of OCS VMR for the specific date (14 March 2010). It is shown that the VMR of OCS increases slightly with time from mid-morning to noon and tends to decrease afternoon. On this particular day, the difference between the maximum and minimum VMR is around 19 pptv (parts per trillion by volume). The decrease about mid-day and late afternoon may correspond to photosynthesis uptake by plants with CO_2 as suggested by White et al. (2010) and Easterly wind may blow OCS or sulphur-containing traces to this region during this day. The hourly and diurnal variation has not been yet understood fully and is open for investigation as it is related to biospheric activity, weather conditions, and others. The sensitivity by the averaging kernel (Fig. 4) and the partial and column amount in Fig. 8 shows that OCS information about its altitude distribution comes from the two regions (troposphere and stratosphere) with the lower troposphere more sensitive for this trace gas as it corresponds to the tropospheric mean mixing ratio of 0.45 ppbv.

Fig. 9 shows the time series of the total column OCS (in molecules/m^2) observed during the measurement period from May 2009 to April 2010. The blank space measurement was taken between 13 June 2009 and 26 November 2009. The total column amount of OCS observed during this period ranges from 5.3×10^{19} to 8.5×10^{19} molecules/m^2 showing seasonal variation. Comparable total column amount observed in our site was observed in the mid-latitude total site in Izana (28^{o}18' N, 16^{o}29' W) on the Canary Island of Tenerife at 2367 m.a.s.l (Schneider, 2002; Krysztofiak et al., 2015) and the work reported by Toon et al. (2018). The seasonal variation of OCS has also been reported by these researchers. In Fig. 10 we got a time series of tropospheric and stratospheric columns together with the ratio of particle concentration in the two regions. The seasonal variation was better observed in this graph with a maximum in a tropospheric amount in May and June (early rainy season) while minimum in December and January (sunny/hot season locally). The stratospheric seasonal variation is the reverse of the tropospheric one as observed from the result. This variation is well revealed on the top panel of the same figure with the ratio of tropospheric to stratospheric total column amount. Total column amount in Wollongong, Australia (southern hemisphere) also shows a seasonal variation with late summer peak and winter trough, from data collected between May 1996 to March 1997 (Griffith et al., 1998; Deutscher et al., 2006). On the other hand, the reduction in troposphere and accession in the stratosphere during the same season may be associated with OCS transport from the free troposphere which occurs mainly through the tropical tropopause layer.

The OCS VMR observed in Fig. 11 also reveals seasonal variation showing the enhanced amount in early summer (May-June) up to 0.6 ppbv which is above the average range of 0.45 – 0.50 ppbv and reduction in December & January, but the specific altitude where the change triggers worth further investigation. The steady declination of OCS in the stratospheric region is observed from the same figure with an average stratospheric mixing ratio of 0.230 ppbv and nearly constant VMR in the troposphere with average VMR of 0.488 ppbv calculated using simple arithmetic mean formula suggested by Chin and Davis (1995) and identifying the mean tropopause and stratopause levels from daily temperature profile of the site obtained from NASA Goddard Earth Observatory system model from 22 May 2009 to 10 January 2010. The two pause levels obtained are 17.12 km and 52.85 km, respectively. This is supported by the work of Engel and Schmidt (1994). The rapid decrease in the stratosphere is related to the oxidation and photolysis sink mechanism there (Deutscher et al., 2006; Chin and Davis, 1993, 1995) where it is converted into background stratospheric sulphate aerosol (Jung layer). Observed values of OCS as reported by different investigators are slightly different. For instance, the tropospheric mixing ratio for OCS reported by Leifer (1989) is 410 pptv with 400 pptv at tropopause level. The result mentioned in Barkley et al. (2008) from space-born observation is that the global tropospheric mean is 0.433 ppbv, and Notholt et al. (2006) confirms that the global mean tropospheric mixing ratio is 0.480-0.520 ppbv; but most investigators reported that the tropospheric OCS mixing ratio is nearly constant and it is about 0.500 ppbv with a latitudinal gradient (Chin and Davis, 1995). Our result deviates by 2.4% of the global mean value. Therefore, the tropospheric mean value of the OCS mixing ratio we obtained is in good agreement with different kinds of literature. The stratospheric mean VMR we found is smaller than the global mean stratospheric VMR of 0.330 ppbv reported by Barkley et al. (2008) from satellite observation. Ignoring the minor contribution from the higher atmosphere (above stratopause) might have contributed to the significant difference between our result and the global mean.

CONCLUSION

In this research, we retrieved atmospheric OCS using 5 microwindows from a ground-based high-resolution FTIR spectrometer installed at Addis Ababa in May 2009 and has been continuously measuring spectra. The vertical profile of OCS shows a minor variation in the troposphere but rapidly decreases with altitude in the stratosphere. The hourly change of column OCS for a date 14th, March 2010 was analysed and shows maximum around noon, and minimum during mid-morning and afternoon with the difference between maximum and minimum to be 0.019 ppbv (19 pptv). This variation may be related to biospheric activity or other pollutants for the city like automobile exhaust gases. The VMR and total column time series from May 2009 to April 2010 shows seasonal variation from 5.3×10^{19} to 8.5×10^{19} molecules/m^2 with the maximum in May and June (early rainy season), and minimum in December and January(hot/sunny season). The mean tropospheric and stratospheric VMR of OCS retrieved from our site is 0.488 ppbv and 0.230 ppbv, respectively, in which the former is comparable to the global average mixing ratio while the latter is significantly smaller than the global mean value reported by Barkley et al. (2008) from satellite observation. The correlation between stratospheric tropopause level and the accession of stratospheric OCS level during hot season worth detail investigation to understand the hourly, diurnal, and seasonal variation of OCS in our region. Data from other nearby sites, satellite, and model are required to validate this result. Besides, long term data from the site is required to study the trend of OCS in the region.

ACKNOWLEDGEMENTS

Our gratitude goes to Dr Thomas Blumenstock from KIT, for his support in the operation of the FTIR spectrometer, training on LINEFIT software, and discussions on the results. We are also grateful to Dr Frank Haze for his patient elaboration of the retrieval code (PROFFIT) and other relevant software, technical support, and discussion of our results. The Institute of Meteorology and Climate Research of Karlsruhe Institute (IMK-KIT) of technology shall also be thanked for financial support to visit the Research Centre in Germany. We also thank NASA/Goddard for daily T, p supply.

REFERENCES

Asaf, D., Rotenberg, E., Tatarinov, F., Dicken, U., Montzka, S. A., & Yakir, D. (2013). Ecosystem photosynthesis inferred from measurements of carbonyl sulphide flux. *Nat. Geosci*., 6(3), 186–190.

Aydin, M., Williams, M. B., Tatum, C., & Saltzman, E. S. (2008). Carbonyl sulphide in air extracted from a South Pole ice core: a 2000 year record. *Atmospheric Chemistry and Physics Discussion*, 7533-7542.

Barkley, M. P., Palmer, P. I., Boone, C. D., Bernath, P. F., & Suntharalingam, P. (2008). Global distributions of carbonyl sulphide in the upper troposphere and stratosphere. *Geophysical Research Letters*, 35, 1-7.

Berry, J., Wolf, A., Campbell, J. E., Baker, I., Blake, N., Blake, D., & Denning, A. S. et al. (2013). A coupled model of the global cycles of carbonyl sulfide and CO_2: A possible new window on the carbon cycle. *J. Geophys. Res. Biogeosci*., 118, 842– 852.

Brühl, C., Lelieveld, J., Crutzen, P. J., & Tost, H. (2012). The role of carbonyl sulphide as a source of stratospheric sulphate aerosol and its impact on climate. *Atom. Chem. Phys*., 12, 1239-1253.

Butcher, S. S., Charlson, R. J., Orians, G. H., & Wolfe, G. V. (1992). Global Biogeochemical Cycles. Academic, London.

Campbell, J., Carmichael, G. R., Chai, T., Mena-Carrasco, M, & Tang, Y. et al. (2008). Photosynthetic control of atmospheric carbonyl sulfide during the growing season. *Science,* 322(5904), 1085–1088.

Crutzen, P. J., Heidt, L. E., Krasnec, J. P., Pollock, W. H., & Seiler, W. (1979). Biomass burning as a source of atmospheric gases: CO, H_2, N_2O, NO, CH_3Cl, and OCS. Nature, 282: 253-256.

Crutzen, P. J. (1976). The possible importance of OCS for the sulphate layer of the stratosphere. *Geophys. Res. Lett.*, 3, 73–76.

Deutscher, N. M., Jones, N. B., Griffith, D. W., Wood, S.W., & Murcray, F.J. (2006). Atmospheric carbonyl sulfide (OCS) variation from 1992-2004 by ground-based solar FTIR spectrometry. *Atmospheric Chemistry and Physics Discussions*, 6 (2), 1619-1636.

Engel, A., & Schmidt, U., (1994). Vertical profile measurements of carbonyl sulfide in the stratosphere. *Geophys. Res. Lett*., 21, 2219–2222.

Griffith, D. W. T., Jones, N. B., McNamara, B., Walsh, C. P., Bell, W., & Bernardo, C. (2003). Intercomparison of NDSC Ground-based Solar FTIR Measurements of Atmospheric Gases at Lauder, New Zealand. *Journal of Atmospheric and Oceanic Technology*, 20, 1138-1153.

Griffith, D. W. T., Jones, N. B., & Matthews, W. A. (1998). Interhemispheric ratio and annual cycle of carbonyl sulfide (OCS) total column from ground-based solar FTIR spectra. *J. Geophys. Res.,* 103, 8447–8454.

Haze, F. (2000). Inversion von spurengasprofilen FTIR-Messungen in Absorption, Dissertation. Genehmigt von der Facultat fur physik der Universitat Karlsruhe (TH), Karlsruhe.

Haze, F., Blumenstock, T., & Paton-Walsh, C. (1999). Analysis of the instrumental line shape of high-resolution Fourier Transform IR spectrometers with gas cell measurements and new retrieval software. *Appl. Opt*., 38, 3417-3422.

Homa, M. G., Tsidu, G. M., & Nega, D. T. (2017). Stratospheric Aerosol Climatology over Ethiopia and Retrieval of it Size Distribution. *Atmos. Chem. Phys. Discuss*. DOI: 10.5194/acp-2017-133.

Johnson, J. E., Bandy, A. R., Thornton, D. C., & Bates, T. S. (1993). Measurements of atmospheric carbonyl sulphide during the NASA chemical instrumentation test and evaluation project: Implications for the global OCS budget, *J. Geophys. Res*., 98, 23443-23448.

Kettle, A. J. (2002). Global budget of atmospheric carbonyl sulfide: Temporal and spatial variations of the dominant sources and sinks. *Journal of Geophysical Research*, 107, D22, 4658.

Kremser, S., Jones, N. B., Palm, M., Lejeune, B., Wang, Y., Smale, D., & Deutscher, N.M. (2015). Positive trends in Southern Hemisphere carbonyl sulphide. *Geophys. Res. Lett*., 42, 9473–9480.

Krysztofiak, G., Té, Y. V., Catoire, V., Berthet, G., & Toon, G. C. et al. (2015). Carbonyl sulfide (OCS) variability with latitude in the atmosphere. *Atmosphere-Ocean*, 53, 89–101.

Kuai, L., Worden, J. R., Campbell, J. E., Kulawik, S. S., Li, K., Lee, M. et al. (2015), Estimate of carbonyl sulphide tropical oceanic surface fluxes using Aura Tropospheric Emission Spectrometer observations, *J. Geophys. Res. Atmos*., 120 (11),012–023. DOI: 10.1002/2015JD023493.

Kuhn, U., & Kesselmeier, J. (2000). Environmental variables controlling the uptake of carbonyl sulphide by lichens. *Journal of Geophysical Research*, 105, 26,783-26,792.

Leifer, R. (1989). Project Airstream: COS measurements in the stratosphere and troposphere. *J. Geophys. Res*., 94, 5173– 5181.

Lejeune, B., Mahieu, E., Vollmer, M. K., Reimann, S., Bernath, P. F. et al. (2016). Optimized approach to retrieve information on atmospheric carbonyl sulfide (OCS) above the Jungfraujoch station and change in its abundance since 1995. *Journal of Quantitative Spectroscopy & Radiative Transfer*, http://dx.doi.org/10.1016/j.jqsrt.2016.06.001.

Main, C., & Davis, D. (1995). A reanalysis of carbonyl sulphide as a source of stratospheric background sulfur aerosol. *Journal of Geophysical Research*, 100: 8993-9005.

Montzka, S. A., Calvert, P., Hall, B. D., Elkins, J. W., Conway, T. J., Tans, P. P. and Sweeney, C. (2007). On the global distribution, seasonality, and budget of atmospheric carbonyl sulfide (COS) and some similarities to CO_2. *J. Geophys. Res*., 112, D09302.

Notholt, J., Weisenstein, D., Kuang, Z., Rhineland, C. P., Toon, G. C. et al. (2003). Composition of the upper tropical troposphere and its influence on the stratospheric aerosol formation. EGS-AGU-EUG Joint Assembly, Vol. 1, p. 4024.

Notholt, J., Toon, G., Jones, N., Griffith, D. and Warneke, T. (2006). Spectral line finding program for atmospheric remote sensing using full radiation transfer. *Journal of Quantitative Spectroscopy and Radiative Transfer*, 97, 112-125.

Rhineland, C. P., Chiou, L., Mahieu, E., Zander, R., Boone, C. D. and Bernath, P. F. (2008). Measurements of long-term changes in atmospheric OCS (Carbonyl sulphide) from infrared solar observations. *Journal of Quantitative Spectroscopy and Radiative Transfer*, 109, 2679-2686.

Rhineland, C. P., Zander, R., Mahieu, E., Demoulin, P., Goldman, A., Ehhalt, D. H., & Rudolph, J. (1992). Ground-Based Infrared Measurements of Carbonyl sulphide Total Column Abundances: Long-Term Trends and Variability. *Journal of Geophysical Research*, 97, 5995-6002.

Rodgers, C. D. (2004). Inverse Methods for Atmospheric Sounding theory and practice. Series on Atmospheric, Oceanic and Planetary physics. World Scientific Publishing, Vol.2, Oxford.

Rothman, L. S., Jacquemart, D., Barbe, A., Benner, D. C., Birk, M., Brown, L. R. et al. (2005). The HITRAN 2004 molecular spectroscopic database. *Journal of Quantitative Spectroscopy and Radiative Transfer*, 96, 139-204.

Rothman, L. S., Gordon, I. E., Barbe, A., Banner, D. C., Bernath, P. F., Birk, M. et al. (2009). The HITRAN 2008 molecular spectroscopic database. *Journal of Quantitative Spectroscopy and Radiative Transfer*, 96, 533-572.

Sandoval-Soto, L., Stanimirov, M., von Hobe, M., Schmitt, V., Valdes, J., Wild, A., & Kesselmeier, J. et al. (2005). Global uptake of carbonyl sulphide (COS) by terrestrial vegetation: Estimates corrected by deposition velocities normalized to the uptake of carbon dioxide (CO2), *Biogeosciences*, 2, 125–132.

Schneider, M. (2002). Continuous Observations of Atmospheric Trace Gases by Ground-based FTIR Spectroscopy at Izana Observatory, Tenerife Island, Ph. D. Dissertation. Institut fur Meteorologie Und Klimaforshung, Karlsruhe.

Seinfeld, J. H., & Pandis, S. N. (2006). Atmospheric Trace Constituents. In J. H. Seinfeld and S. N. Pandis (Eds.), *Atmospheric Chemistry and Physics: From Air Pollution to Climate Change* (pp.18-68), 2nd edition. Wiley.

Steinbacher, M., Bingemer, H. G., & Schmidt, U. (2004). Measurements of the exchange of carbonyl sulfide (OCS) and carbon disulfide (CS_2) between soil and atmosphere in a spruce forest in central Germany. *Atmos. Environ*., 38(35), 6043– 6052.

Sung, K., Skelton, R., Walker, K. A., Boone, C. D., Fu, D., & Bernath, P. F. (2007). N_2O and O_3 arctic olumn amounts from PARIS-IR observations: Retrievals, characterization and error analysis. *Journal of Quantitative Spectroscopy and Radiative Transfer*, 107, 385-406.

Toon, G. C., Jean-Francois, L. B., & Sung, K. (2018). Atmospheric carbonyl sulfide (OCS) measured remotely by FTIR solar absorption spectrometry. *Atmos. Chem. Phys*., 18, 1923–1944.

Turco, R. P., Whitten, R. C., Toon, O. B., Pollack, J. B., & Hamill, P. (1980). Stratospheric aerosols and climate. *Nature*, 283, 283–285.

Twomy, S. (1977). *Introduction to the Mathematics of Inversion in Remote Sensing and Indirect Measurements*. Dover Publications, Inc.

Waiacek, A., Taylor, J. R., Strong, K., Saari, R., Kertzenmacher, T. E., Jones, N. B., & Griffith, D. W. T. (2007). Ground-Based Solar Absorption FTIR Spectroscopy: Characterization of Retrievals and First Results from a Novel Optical Design Instrument at a new NDACC Complementary Station. *Journal of Atmospheric and Oceanic Technology*, 24(3), 432-448.

Watts, S. F. (2000). The mass budget of carbonyl sulfide, dimethyl sulfide, carbon disulfide and hydrogen sulfide. *Atmospheric Environment*, 10, 761-779.

White, M. L., Zhou, Y., Russo, R. S., Mao, H., Talbot, R., Varner, R. K., & Sive, B. C. (2010). Carbonyl sulphide exchange in a temperate loblolly pine forest grown under ambient and elevated CO_2. *Atmos. Chem. Phys*., 10, 547-561.